




Topical Review

Recent research trends in textile-based temperature sensors: a mini review

Heebo Ha^{1,5}, Thirumalaisamy Suryaprabha^{1,5}, Chunghyeon Choi^{1,5},
Zubair Ahmed Chandio², Byungjin Kim^{3,6}, Sooman Lim^{4,*} ,
Jun Young Cheong^{2,*}  and Byungil Hwang^{1,*} 

¹ School of Integrative Engineering, Chung-Ang University, Seoul 06974, Republic of Korea

² Bavarian Center for Battery Technology (BayBatt) and Department of Chemistry, University of Bayreuth, Universitätsstraße 30, D-95447 Bayreuth, Germany

³ Department of Mechanical Engineering, Ulsan National Institute of Science and Technology (UNIST), Ulsan 44919, Republic of Korea

⁴ Department of Flexible and Printable Electronics, LANL-JBNU Engineering Institute, Jeonbuk National University, Jeonju, Republic of Korea

E-mail: smlim@jbnu.ac.kr, Jun.Cheong@uni-bayreuth.de and bihwang@cau.ac.kr

Received 15 April 2023, revised 4 July 2023

Accepted for publication 20 July 2023

Published 22 August 2023



CrossMark

Abstract

In this review, the current state of research on textile-based temperature sensors is explored by focusing on their potential use in various applications. The textile-based sensors show various advantages including flexibility, conformability and seamlessness for the wearer. Integration of the textile-based sensors into clothes or fabric-based products enables continuous and sensitive monitoring of change in temperature, which can be used for various medical and fitness applications. However, there are lacks of comprehensive review on the textile-based temperature sensors. This review introduces various types of textile-based temperature sensors, including resistive, thermoelectric and fibre-optical sensors. In addition, the challenges that need to be addressed to fully realise their potential, which include improving sensitivity and accuracy, integrating wireless communication capabilities, and developing low-cost fabrication techniques. The technological advances in textile-based temperature sensors to overcome the limitations will revolutionize wearable devices requiring function of temperature monitoring.

Keywords: fibre, flexible, sensor

(Some figures may appear in colour only in the online journal)

1. Introduction

Temperature sensors are devices that convert various physical changes caused by changes in temperature into electrical signals. Temperature sensors are classified in various ways depending on principles and materials, such as resistance temperature detectors (RTDs), infrared temperature sensors, and thermocouples. Materials such as metal, metal oxide, and ceramic, which have limited characteristics including inflexibility, heavyweight, and fragility, have been mainly used to make temperature sensors [1–3]. Recently, carbon-based

⁵ These authors contributed equally to this work.

⁶ Present address: Hanwha Chemical, 14, Jindallae-gil, Yeosu-si 59614, Republic of Korea.

* Authors to whom any correspondence should be addressed.



Original content from this work may be used under the terms of the [Creative Commons Attribution 4.0 licence](https://creativecommons.org/licenses/by/4.0/). Any further distribution of this work must maintain attribution to the author(s) and the title of the work, journal citation and DOI.



Figure 1. Schematic illustration of the substrate materials for parts of flexible sensors. Clockwise from top right: polyimide (PI), polyurethane, pectin, silk, cellulose, paper, ecoflex, and polydimethylsiloxane. Reproduced from [34] under the Creative Commons Attribution 4.0 International (CC BY 4.0) Licence.

materials, like carbon black, graphene, and carbon nanotube, and various flexible substrates, like polydimethylsiloxane (PDMS), textile, and polyimide (PI), have been studied to get better mechanical and electrical properties [4–9]. Fabrication methods for temperature sensors vary depending on the sensor type and application and they include thin-film deposition, printing, coating, etc [1, 10, 11]. Temperature sensors are essential components in various fields, including healthcare, sports and the manufacturing industry [12–17].

With the unique properties such as flexibility, lightweight, and seamlessness to the human body, textile-based temperature sensors have emerged as a promising technology, especially in wearable electronics [18–21]. In addition, the potential of textile-based temperature sensors is expected to revolutionise healthcare by enabling continuous and non-invasive monitoring of patients' body temperature, thereby improving patient care and reducing the costs for healthcare process [22–24].

The development of textile-based temperature sensors requires the integration of various types of materials, electronic components, and manufacturing technologies [13–15, 23]. Therefore, developing the innovative technologies in each part is important to produce the high quality

temperature sensors. For examples, the sensitivity and accuracy of the sensors can be improved through the innovative materials including conductive textiles, which can be integrated as temperature sensors with high sensitivity and accuracy [25–27]. In addition, advances in electronic components enables the miniaturisation of devices such as low-power temperature sensors that help to realize commercial wearable devices [28–30]. The progression of manufacturing technologies can allow the mass production of textile-based temperature sensors with high precision and reproducibility [31–33].

The design of textile-based temperature sensors is critical to their performance and reliability. Design considerations include the choice of materials, sensor configuration and data-processing techniques. The choice of materials is important because materials determine the sensitivity and accuracy of temperature sensors (figure 1) [34]. Further, the sensor configuration can affect the spatial resolution and response time of a sensor. Finally, data-processing techniques are necessary to filter out noise and extract meaningful information from sensor data.

Fabrication methods for textile-based temperature sensors have also been a focus of research [31, 34–36]. Weaving,

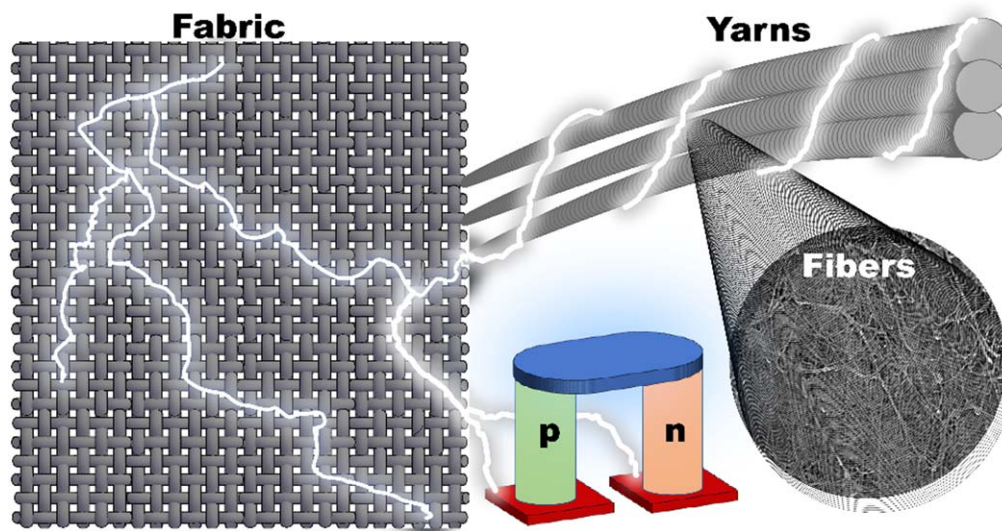


Figure 2. Schematic of TE-based textile temperature sensor. Reproduced from [47] under the Creative Commons Attribution 4.0 International (CC BY 4.0) Licence.

printing, and embroidery are some of the techniques that have been used to fabricate temperature sensors in textiles [13, 15, 16, 19, 23, 25, 28, 32]. Weaving is a popular method because it can produce sensors having high resolution and durability. Printing and embroidery are also attractive options because they can produce sensors having high flexibility and conformability.

The applications of textile-based temperature sensors are diverse and rapidly expanding [37, 38]. In healthcare, textile-based temperature sensors have been used to monitor the body temperature of patients, particularly those with fever or hypothermia [39, 40]. In addition, textile-based temperature sensors are now widely used in sports, where the core body temperature of athletes during exercise is monitored to help prevent heat exhaustion and other heat-related illnesses [41, 42]. Furthermore, textile-based temperature sensors are equipped in various industrial devices that measure the change in temperature of machinery, equipment and materials, thereby improving the controllability of process, safety, and efficiency [43, 44]. In addition, apparels with the textile-based temperature sensors can control the thermal properties of clothing and other textiles, thereby improving comfort and energy efficiency of clothes [45, 46].

In this review, a comprehensive overview of the recent advances in textile-based temperature sensors is summarized. The recent developments in materials, applications and manufacturing technologies for textile-based temperature sensors is discussed. Each factors including the choice of materials, sensor configuration and data-processing techniques that can improve the properties of the textile-based temperature sensors is summarized. Furthermore, various fabrication methods that have been used to produce textile-based temperature sensors, including weaving, printing and embroidery, are introduced. Finally, the various applications of textile-based temperature sensors in healthcare, sports, industrial applications and smart textiles are discussed, which

provides a perspective for the potential of textile-based temperature sensors for future developments in this rapidly evolving field.

2. Types of temperature sensors

2.1. Thermoelectric-powered textile-based temperature sensors

There are several types of textile-based temperature sensors [47]. One type is a thermoelectric-powered textile-based temperature sensor (figure 2) [47]. For the sensors, thermoelectric (TE) materials and electrodes are coated or printed on the surface of textiles. Thermoelectric-powered textile-based temperature sensors are flexible and lightweight sensors that can be used in wearable electronic skin because of their three-dimensional (3D) conformability and breathability. These sensors comprise thermoelectric segments that convert temperature differences into an electrical voltage. The sensitivity of these sensors is low because of the low integration density of thermoelectric (TE) segments. These sensors typically comprise a thermoelectric generator (TEG) integrated into a textile substrate, along with temperature-sensing elements such as thermistors or resistive temperature sensors. When the temperature of the TEG changes, it generates a voltage that can be used to power the temperature-sensing elements. This approach eliminates the need for batteries or external power sources, making thermoelectric-powered textile-based temperature sensors ideal for wearable technology and other applications in which portability and flexibility are essential.

Various recent researches have explored the development of the textile-based temperature sensors using thermoelectric materials [37, 38]. For example, Liu *et al.*, developed a thermoelectric-powered wearable temperature sensor using a

Table 1. Thermoelectric-powered textile-based temperature sensors feature comparison.

Material	Fabrication method	Comments	Output voltage	References
Silver selenide (Ag ₂ Se), polyvinylpyrrolidone (PVP)	Screen printing	Low flexibility when PVP content is low	21.6 mV at $\Delta 40$ K	[48]
Indium oxide (In ₂ O ₃), indium tin oxide (ITO)	Screen printing	High Seebeck coefficient	—	[49]
Copper (Cu) cellulose	Electroless metal deposition	Good durability	0.4 mV at $\Delta 71$ K	[28]
Poly(3,4-ethylenedioxythiophene):poly(styrenesulfonate) (PEDOT: PSS), 3D spacer fabric (SF)	Soaking	Can measure pressure and temperature simultaneously with high sensitivity and accuracy	203 mV at $\Delta 40$ K	[50]
Semiconducting glass of Cu–As–Te–Se system, polyetherimide (PEI)	Sealed-ampoule melt- quenching	High flexibility	3.5 mV at $\Delta 70$ K	[51]

flexible polymer substrate made from PI, a TEG made from silver selenide (Ag_2Se)-based thermoelectric materials, and polyvinylpyrrolidone (PVP) as an addition of binder [48]. Ag_2Se /PVP films were deposited by screen printing. The relationship between temperature difference and voltage was linear (figure 3(A)). The output voltages of TEG were 11.1 mV and 21.6 mV at the temperature differences of 20 K and 40 K respectively (figure 3(B)). The voltages of 1.7 mV and 7.3 mV were measured at temperature differences of 4 K and 15 K, respectively, which indicates that their film has the potential to be used for wearable devices (figures 3(C)–(D)). In the other work by Liu *et al.*, a flexible, thermoelectric-powered temperature sensor using a TEG made from $\text{In}_2\text{O}_3/\text{Cu}$ was demonstrated [49]. The longer the heat treatment was performed, the better performance was shown (figure 3(F)). Sensitivity reached up to $175 \mu\text{V}^\circ\text{C}^{-1}$ after 3 h of heat treatment. They made a flexible temperature sensor composed of In_2O_3 and ITO using the screen printing method. The sensor demonstrated high sensitivity of $162 \mu\text{V}^\circ\text{C}^{-1}$ (figure 3(G)). It also maintained excellent working stability and reliability at various temperatures below 199°C (figure 3(H)).

Landsiedel *et al.* demonstrated a flexible thermoelectric sensor matrix, which was constructed by electroless deposition of copper layers on cellulose fabric [28]. When the temperature difference was 71 K, the average voltage was 0.4 mV. Using aluminium as the second material, a thermoelectric coefficient of $3\text{--}4 \mu\text{V K}^{-1}$ was realised, which is sufficient for manufacturing textile-based temperature measurement devices (figures 4(A)–(G)). Further, Li *et al.* demonstrated a large-area, wearable, self-powered pressure-temperature sensor based on 3D thermoelectric spacer fabric [50]. They used poly(3,4-ethylenedioxythiophene):poly(styrenesulfonate) (PEDOT:PSS) as an organic thermoelectric material. The sensor can measure pressure and temperature simultaneously with high sensitivity and accuracy. The output voltage at the temperature difference of 40 K reached 203 mV for the device with 100 units. The working stability was so excellent that the output voltage remained stable for a long time. The LED could also be lit by harvesting energy from body temperature (figures 4(H)–(L)).

Zhang *et al.* demonstrated thermoelectric fibre sensor containing a semiconducting glass of the quaternary Cu–As–Te–Se system as core and a polymer cladding of poly(etherimide) (PEI) [51]. The semiconducting glass rod was synthesized by a standard sealed-ampoule technique. It showed high mechanical flexibility owing to the presence of PEI cladding. Sensitivity and accuracy were comparable with commercial temperature sensors. The response time was so fast that it was less than 3 s, and the temperature sensing performance did not fall even when wrapped around a glass rod with radius of 3 mm (figures 5(A)–(I)).

Thermoelectric-powered textile-based temperature sensors offer several advantages over traditional battery-powered sensors, including greater portability, flexibility and scalability. Additionally, they are more environment friendly because they do not require disposable batteries. As research in this field continues, thermoelectric-powered sensors are

likely to become increasingly common in wearable technology and other applications in which flexibility and portability are essential. The contents of thermoelectric-powered textile-based temperature sensors are summarized in table 1.

2.2. Textile-based resistive temperature sensors

Another type of textile-based temperature sensor is a resistive temperature sensor. These sensors are made by coating or printing conductive materials on textiles (figure 6) [52]. The resistance of the conductive material changes with temperature, enabling the sensor to detect temperature changes. Pure metals are commonly used as thermal resistance materials. Since the kinetic energy of free electrons increases, the resistance tends to increase as the temperature increases. As the temperature rises, the movement of electrons changes, which increases the energy required for directional movement. This leads to an increase in resistance. This is described as follows:

$$R_t = R_0 [1 + \alpha(t - t_0)], \quad (1)$$

where R_t and R_0 is the resistance value at time t and t_0 , respectively, α represents the temperature coefficient of resistance material [53, 54]. Thus, the resistance sensitivity can be represented as:

$$K = R_0^{-1} dR_t/dt = \alpha. \quad (2)$$

The temperature coefficient varies with temperature and only be regarded as a constant within a certain temperature range.

A textile-based resistive temperature sensor is a type of sensor that can be integrated into fabrics to measure temperature changes. It comprises conductive threads or yarns of metals such as silver or copper, which are woven into the fabric in a way that generates temperature-dependent resistance. When the temperature changes, the resistance of the conductive thread changes as well, and this change can be measured to determine the temperature. This makes textile-based resistive temperature sensors an excellent choice for applications that require temperature monitoring, such as in wearable technology, medical monitoring and smart home systems.

Lugoda *et al.* developed a wearable temperature sensor based on conductive polymer composite yarns [52]. The sensor was integrated into an armband and demonstrated high sensitivity to temperature changes, with a response time of less than 10 s (figures 7(a)–(d)) [52]. Dakoco *et al.* demonstrated a textile-based temperature sensor fabricated through inkjet printing technology (figures 7(E)–(F)) [11]. The sensor exhibited high accuracy, with a resolution of 0.1°C (figure 7(G)), and it could be integrated into fabrics using standard textile-manufacturing processes. In the work of Liu *et al.*, Ni-coated textile was used to fabricate a temperature sensor [55]. The sensor demonstrated high sensitivity to temperature changes, with a linear response over a wide temperature range (figures 8(a)–(d)). Fromme *et al.* fabricated e-textile with metal nanocoating pattern by using a laser welding technology (figure 8(e)) [56]. They used a copper-welded textile as a resistive temperature

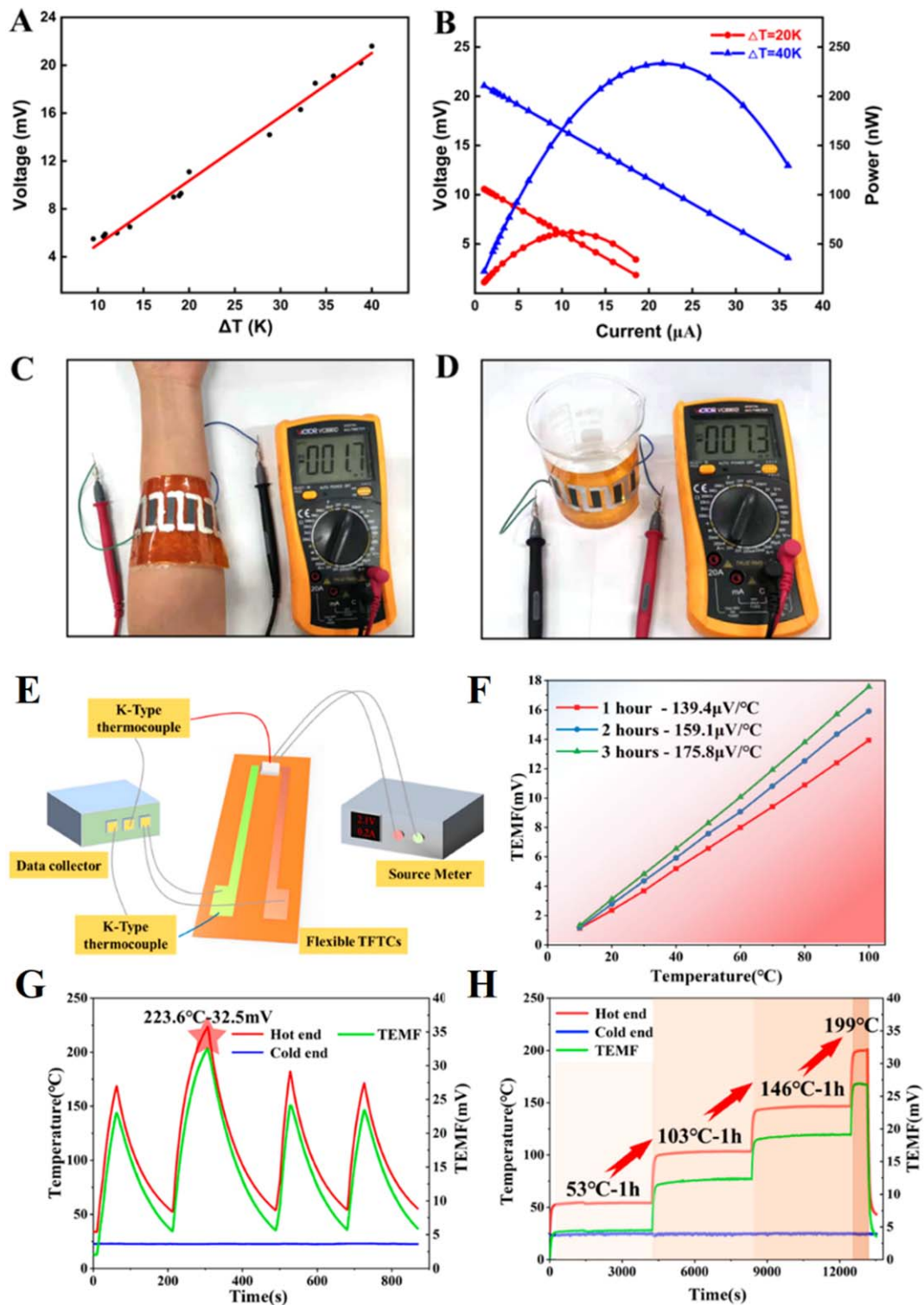


Figure 3. (A) Open voltage changes in PI30 F-TEG with ΔT . (B) Relationship between the output voltage and current and power at $\Delta T = 20$ and 40 K. (C) Voltage generated (1.7 mV) by ΔT between the arm and the environment. (D) Voltage generated (7.3 mV) by ΔT between the upper (cold) and lower (hot) surfaces of the beaker. Reproduced from [48] under the Creative Commons Attribution 4.0 International (CC BY 4.0) Licence. Comprehensive evaluation of sensor performance: (E) self-designed calibration test system of sensor. (F) Comparison of the thermoelectric characteristics of the different thermocouples (In_2O_3/Cu) (In_2O_3 thermo-electrode under different heat-treatment periods). The optimised sensitivity of the In_2O_3 thermo-electrode was $175.8 \mu V/^{\circ}C$, (G) Evaluation of test repeatability of sensors prepared by screen-printing technology (In_2O_3/ITO). The highest instantaneous temperature measured was $223.6^{\circ}C$. (H) Temperature retention of the sensor that was tested at different temperatures. The heat preservation test was performed at $53^{\circ}C$, $103^{\circ}C$ and $146^{\circ}C$, respectively, for up to 1 h. In addition, a short-term test of 10 min was performed at $\sim 199^{\circ}C$. Reproduced from [49] under the Creative Commons Attribution 4.0 International (CC BY 4.0) Licence.

Table 2. Textile-based resistive temperature sensors feature comparison.

Material	Fabrication method	Comments	Temperature coefficient of resistance	References
Titanium (Ti)/ Gold (Au), polyimide (PI)	Knit braiding, braiding, double covering	Not affected by bending	$2.24 \times 10^{-3} \text{ }^{\circ}\text{C}^{-1}$ (knit braiding) $1.53 \times 10^{-3} \text{ }^{\circ}\text{C}^{-1}$ (braiding) $2.58 \times 10^{-3} \text{ }^{\circ}\text{C}^{-1}$ (Double covering)	[52]
Gold (Au), polyimide (PI)	Inkjet printing	Good sensitivity	$2.19 \times 10^{-3} \text{ }^{\circ}\text{C}^{-1}$	[11]
Nickel (Ni), Polytetrafluoroethylene (PTFE)	Weaving	Power-free multifunctional	$1.1 \times 10^{-2} \text{ }^{\circ}\text{C}^{-1}$	[55]
Copper (Cu), polyethersulfon-cotton woven fabric	Laser welding	High durability	$3.9 \times 10^{-3} \text{ }^{\circ}\text{C}^{-1}$	[56]

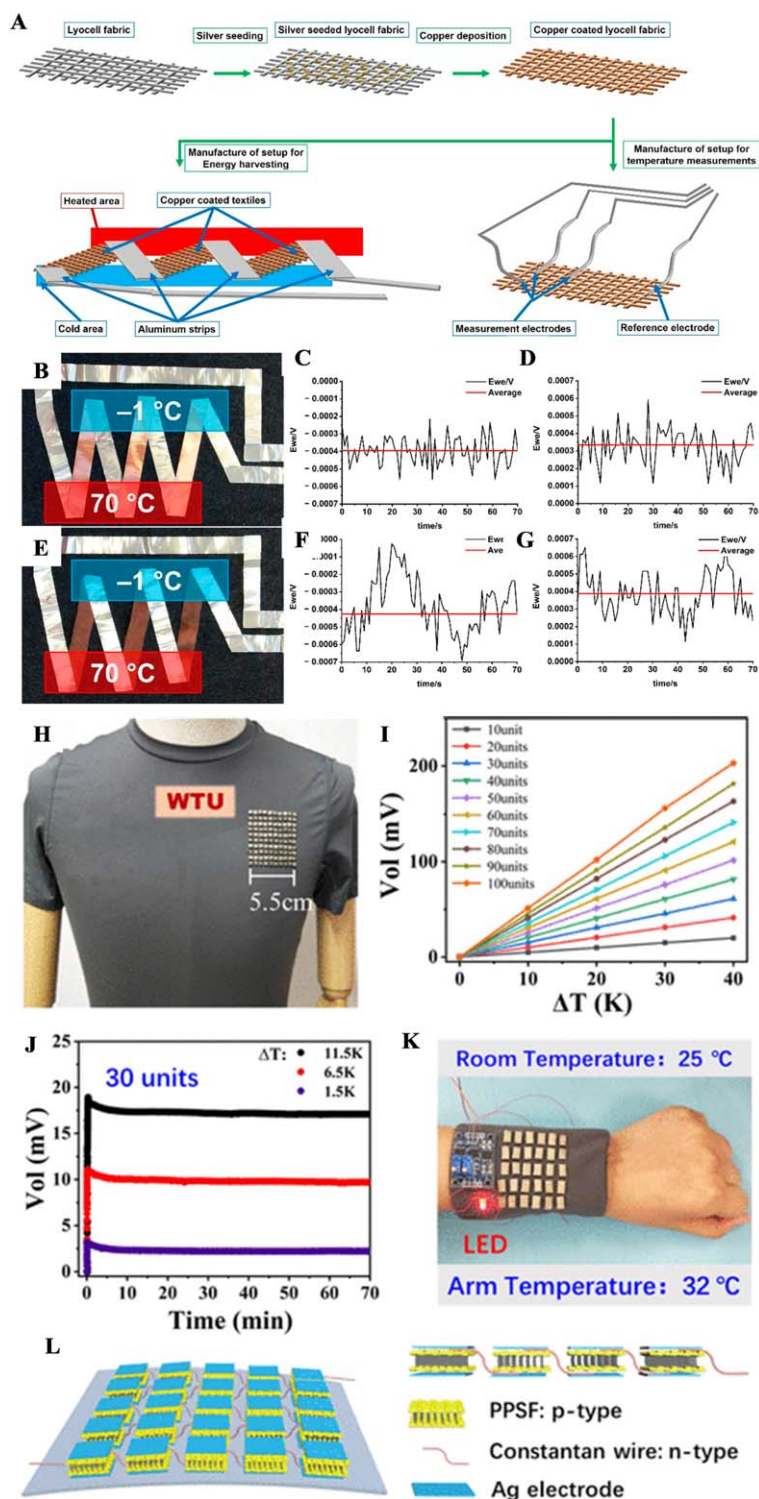


Figure 4. (A) Manufacture of textile-based thermocouples usable for temperature measurements and energy harvesting, made from copper-coated lyocell fabrics. Thermoelectric output voltages of arrangements of three thermocouples in series using strips of copper and aluminium foils (B–D) and strips of copper-coated textiles and aluminium foils (E–G). Temperature difference = 71 K: (C) Cu-strips + Al-strips, (D) same arrangement with reverted temperature gradient, (F) Cu-coated textile + Al-strips and (G) same arrangement with reverted temperature gradient. Reproduced from [28] under the Creative Commons Attribution 4.0 International (CC BY 4.0) Licence. (H) Photograph of the PEDOT:PSS/3D spacer fabric (PPSF)-based TEG containing 100 units: (I) voltages generated by the PPSF-based thermoelectric device containing a different number of units (4 mm × 4 mm in area) versus ΔT , (J) generated voltage stability of the PPSF thermoelectric devices containing 30 units, (K) light-emitting diode lit using the PPSF thermoelectric devices under environmental conditions (ΔT equals the temperature difference between human skin and the surrounding environment) and (L) construction of the thermoelectric device. Reproduced with permission from [50]. Copyright 2020 American Chemical Society.

Table 3. Fibre optic temperature sensors feature comparison.

Sensor category	Material	Fabrication method	Sensitivity	References
FBG sensor	Polyetherimide (PEI), glass fibre	Embedding	—	[57]
	E-glass fibre (GF), carbon fibre (CF)	Embedding	11.9 pm °C ⁻¹ for GF 19.1 pm °C ⁻¹ for CF	[58]
Raman scattering sensor	Carbon nanotube, epoxy resin	—	—	[35]
Fluorescence-based sensor	PbS@CdS@CdS QDs, Silica nanoparticles	Microemulsion	0.2% K ⁻¹	[59]
SPR sensor	Titanium dioxide (TiO ₂), gold (Au)	—	6038.53 nm RIU ⁻¹ , -2.40 nm °C ⁻¹	[60]
Clad modified fibre optic sensor	ZnO, Al ₂ O ₃ , SnO ₂ , TiO ₂	Co-precipitation	~27 for Al ₂ O ₃	[61]
	Al ₂ O ₃ , MgO	Co-precipitation	~10.8 for Al ₂ O ₃ -MgO (50%–50%)	[62]

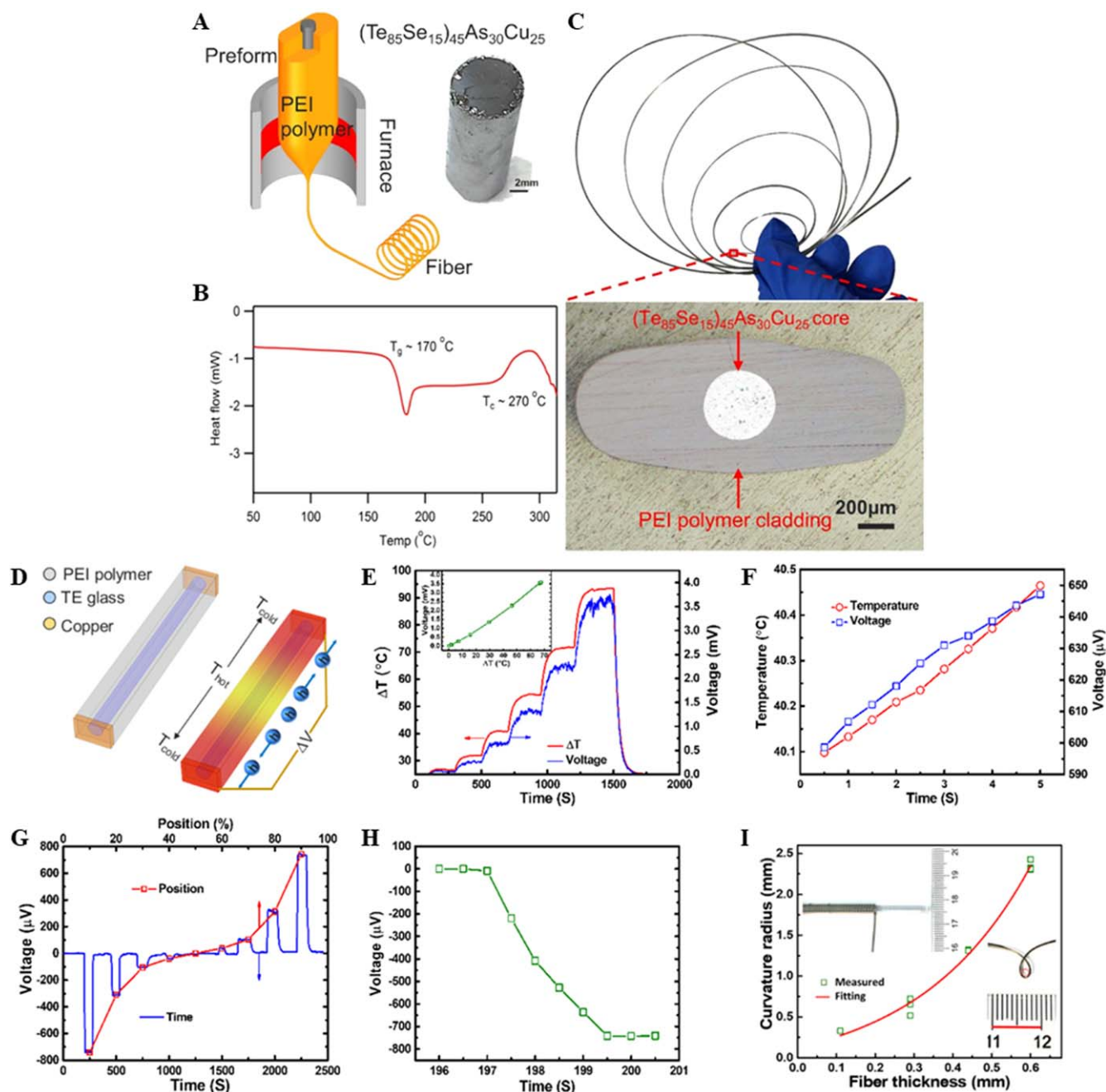


Figure 5. (A) Schematic of the thermal drawing process of a TE fibre from the semiconducting glass and PEI polymer. (B) Glass-transition temperature (T_g) and crystallization temperature (T_c) of the semiconducting glass measured by DSC. (C) Single TE fibre and the cross section optical microscope image of fibre. (D) Schematic of the measuring process for the thermal sensing performance of the TE fibre. (E) Real-time recording of the temperature of the heat source located at the 20% length of the whole fibre via the corresponding output voltage from the temperature difference at two fibre ends. (F) Thermal sensor's temperature resolution. (G) Real-time output voltages from different positions of the thermal sensor. (H) Sensitivity of the thermal sensor via finger touching. (I) Minimum curvature radius of TE fibres with different fibre thicknesses, and the inset shows that the TE fibre is flexible enough to be wrapped on the surface of a 3 mm diameter silica rod. Reproduced with permission from [51]. Copyright 2018 American Chemical Society.

sensor. The temperature sensor exhibited a linear relationship to temperature and the accuracy of the sensor was $\pm 1^\circ\text{C}$ from 25°C – 60°C , $\pm 2^\circ\text{C}$ to 100°C , and $\pm 7.5^\circ\text{C}$ for a temperature higher than 140°C (figure 8(f)). The authors suggested that these sensors could be used in various applications, including smart textiles and wearable electronics. Overall, the textile-based resistive temperature sensors have demonstrated the potential to be used for a

wide range of applications, including wearable technology, medical monitoring and smart home systems. The use of conductive fibres and yarns offers a highly scalable and flexible approach to temperature sensing, with the ability to integrate sensors directly into fabrics during the manufacturing process. The features of the textile-based resistive temperature sensors described above are summarized in table 2.

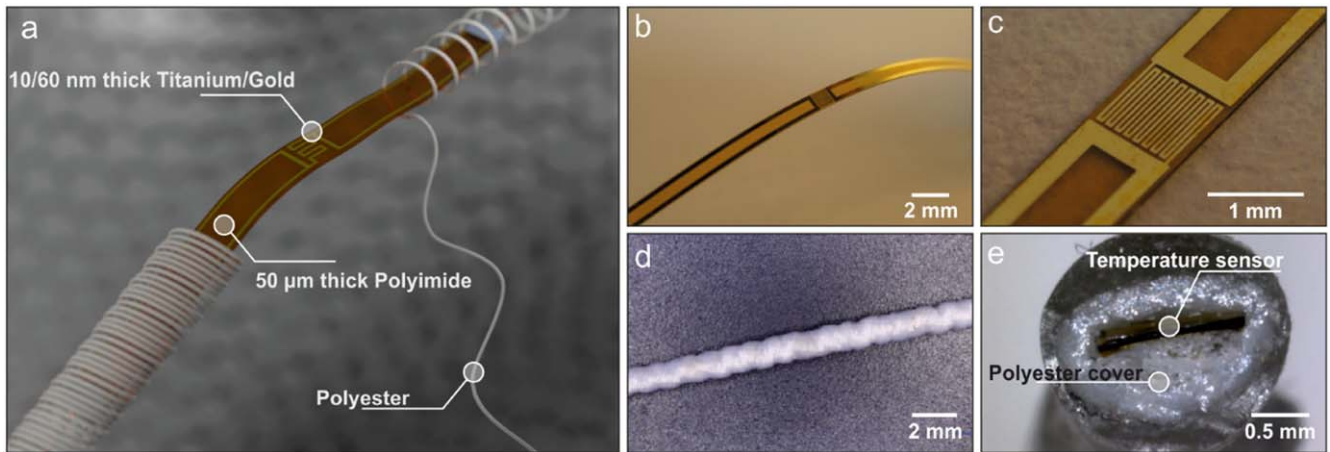


Figure 6. (a) Concept of the flexible temperature sensor embedded within the fibres of a textile yarn. (b) Bending of the uncovered flexible resistance temperature detectors (RTD). (c) Close-up of the sensing area of the RTD. (d) RTD embedded within a braided polyester yarn. (e) Cross section of the braided temperature-sensing yarn (Epoxy resin was utilised to harden the yarn to produce a clean cut). Reproduced from [52] under the Creative Commons Attribution 4.0 International (CC BY 4.0) Licence.

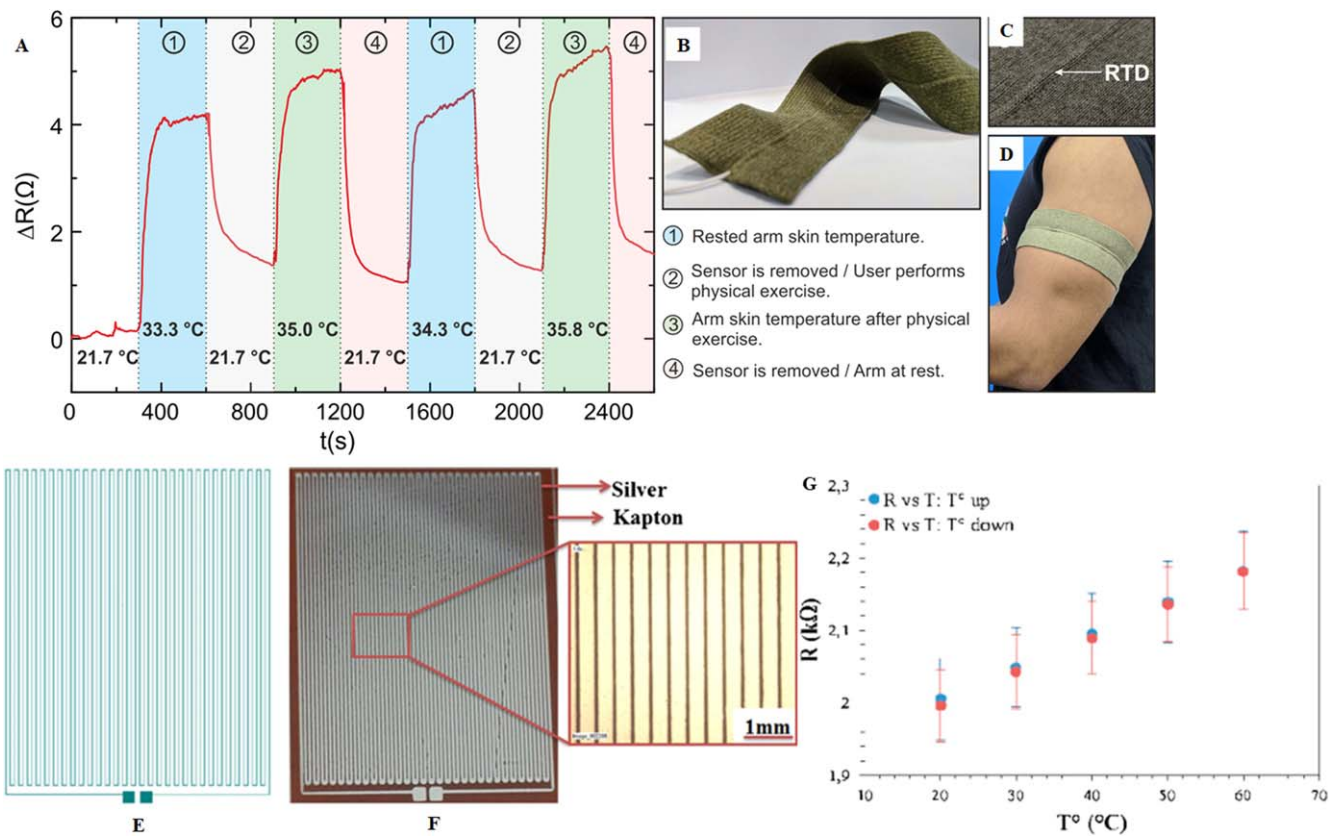


Figure 7. (A) Temperature measurements obtained from the temperature-sensing yarn positioned within the armband during a preliminary user trial. (B) Prototype armband with the temperature-sensing yarn positioned at the centre. (C) Close-up image of the sensing area of the armband. (D) Armband worn on the upper arm. Reproduced from [52] under the Creative Commons Attribution 4.0 International (CC BY 4.0) Licence. Photographs of the (E) designed temperature sensor and (F) inkjet-printer-printed silver temperature sensor on Kapton substrate. (G) Resistance versus temperature of the printed temperature sensor over time. Reproduced with permission from [11]. Copyright 2016 Elsevier.

2.3. Fibre optic temperature sensors

Fibre optic temperature sensors are also representative temperature sensors that can be incorporated into textiles (figure 9). In fibre optic temperature sensors, optical fibres

that can detect changes in temperature are used. The thermal gradient results in a change in optical properties of the fibre, which can be converted into the degree of temperature change [36]. These sensors typically comprise a length of optical fibre that is coated with a thermally sensitive material or has a

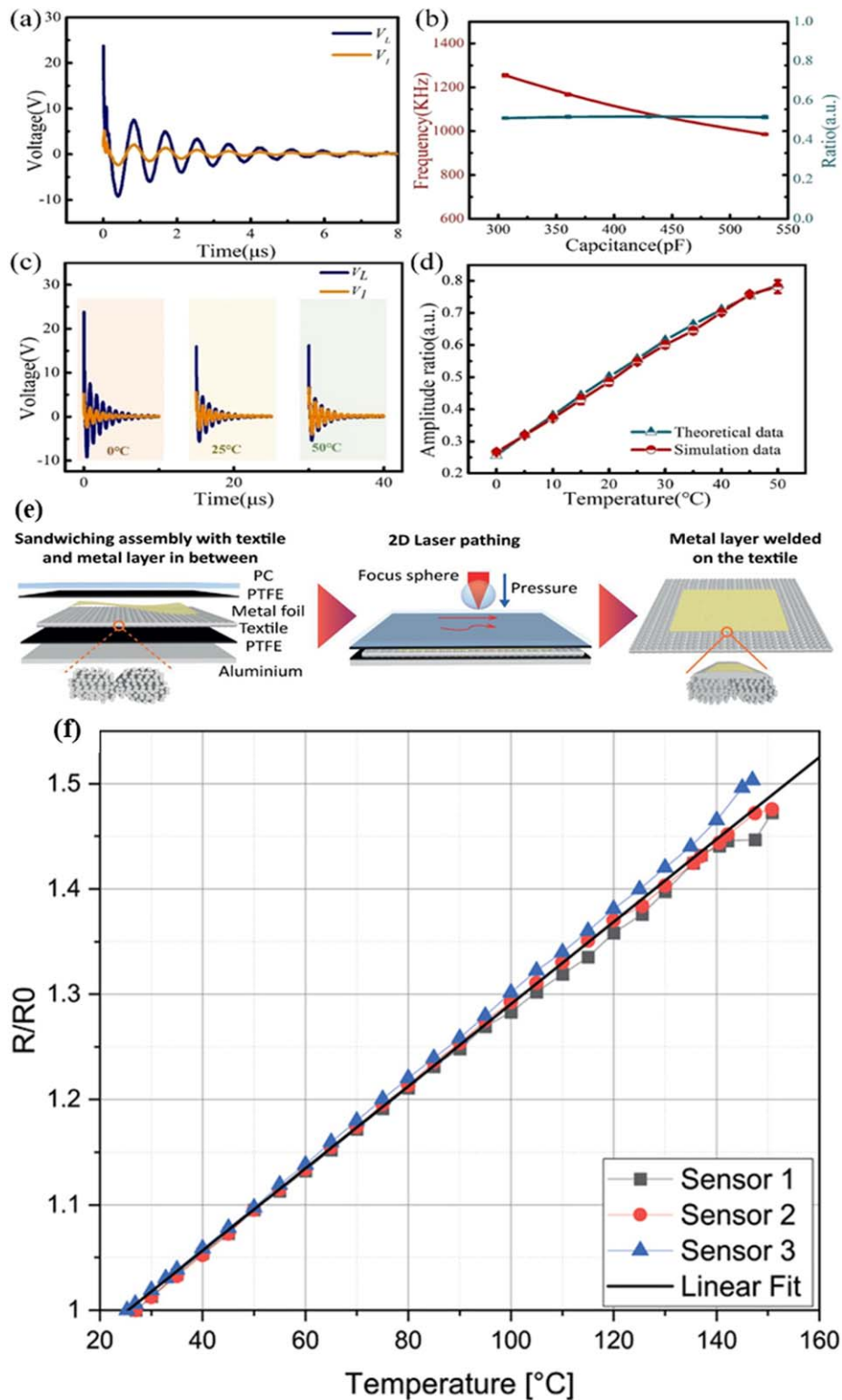


Figure 8. Characterisation of temperature sensing. (a) Measured voltage across R_1 and the entire branch that exists at 0°C , (b) calculated f_r and ratio r corresponding to different capacitance loads ($C_1 = 20\text{ pF}$, $L = 47\ \mu\text{H}$), (c) output voltage across L and R_1 at 0°C , 25°C and 50°C and (d) calibrated ratio r at each temperature ranging from 0°C to 50°C . Reproduced with permission from [55]. Copyright 2022 Elsevier. (e) Schematic of the laser welding process from the sandwich assembly to the laser pathing while applying pressure and with the metal layer welded onto the textile. (f) The temperature sensors' resistivity ratio over temperature change. Reproduced with permission from [56]. Copyright 2021 The Author. Advanced Electronic Materials published by Wiley-VCH GmbH.

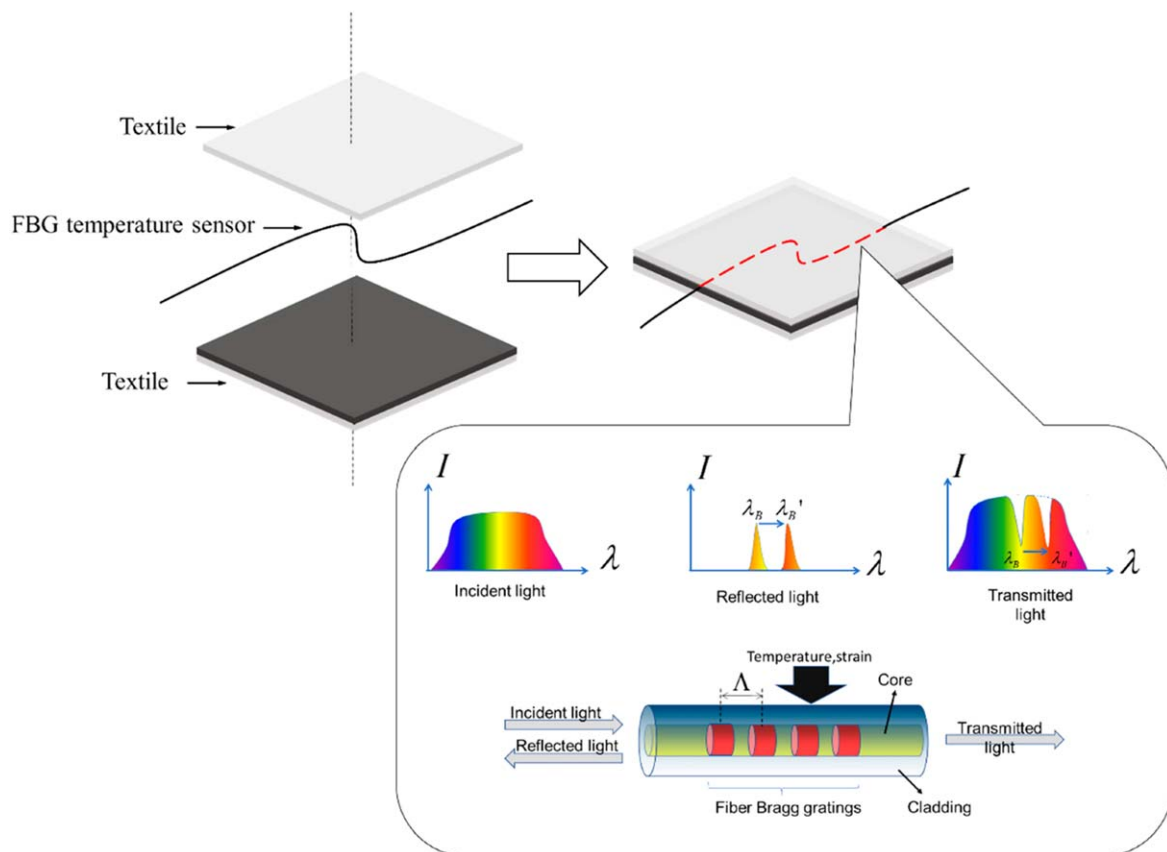


Figure 9. Working mechanism of fibre Bragg grating (FBG) temperature sensors for textile application. Reproduced from [36] under the Creative Commons Attribution 4.0 International (CC BY 4.0) Licence.

temperature-sensitive element attached to it. As temperature changes, the optical properties of the fibre change, causing changes in light transmission that can be measured to determine the temperature. Fibre optic temperature sensors offer several advantages over traditional temperature sensors, including high accuracy, fast response times and immunity to electromagnetic interference. In addition, they are highly versatile and can be used in a wide range of industrial areas, including aerospace, automotive and medical monitoring. Fibre optic temperature sensors have many applications such as monitoring in nuclear magnetic resonance imaging and radio-frequency energy environments, structural health monitoring, aerospace, metallurgy, fossil fuels, power production, industrial processing plants, bridges, tunnels, mines, buildings and oil and gas pipelines.

There are several types of fibre optic temperature sensors, including distributed and point sensors. In distributed sensors, optical fibres that are specially designed to allow temperature changes to be measured along the entire length of the fibre are used. The temperature changes in large structures such as pipelines or bridges can be detected with such temperature sensors, and they are particularly useful for monitoring temperature gradients or hot spots. By contrast, point sensors use a small section of an optical fibre that is coated with a temperature-sensitive material or has a temperature-sensitive element attached to it. The point sensors can measure temperature changes at specific application areas, such as in

wearable electronic components or medical implants. Depending on the sensing system, the temperature sensors are categorised as fibre Bragg grating (FBG) sensors, Raman scattering sensors, fluorescence-based sensors, surface plasmon resonance (SPR) sensors or clad modified fibre optic sensor.

FBG sensors use a length of optical fibre that is inscribed with a periodic pattern of refractive index variations. As the temperature changes, the periodicity of the pattern changes, causing a shift in the wavelength of the reflected light. By measuring this wavelength shift, the temperature can be determined. FBG sensors are highly accurate and can be used in a wide range of applications in fields such as aerospace, oil and gas and civil engineering. Chen *et al.* proposed a new FBG sensor having a complex woven structure [57]. Glass fibre-reinforcement was integrated with a polyetherimide matrix (figures 10(a)–(d)), which enabled high mechanical stability [57]. Jenkins *et al.* demonstrated composite-based FBG sensors that could detect a temperature gradient (figures 10(e)–(f)) [58].

Raman scattering sensors use a length of optical fibre that is coated with a temperature-sensitive material. As temperature changes, the material undergoes a phase transition, causing a shift in the frequency of the Raman-scattered light. By measuring this frequency shift, the temperature can be determined. Raman scattering sensors are highly sensitive and can be used in applications such as medical monitoring and

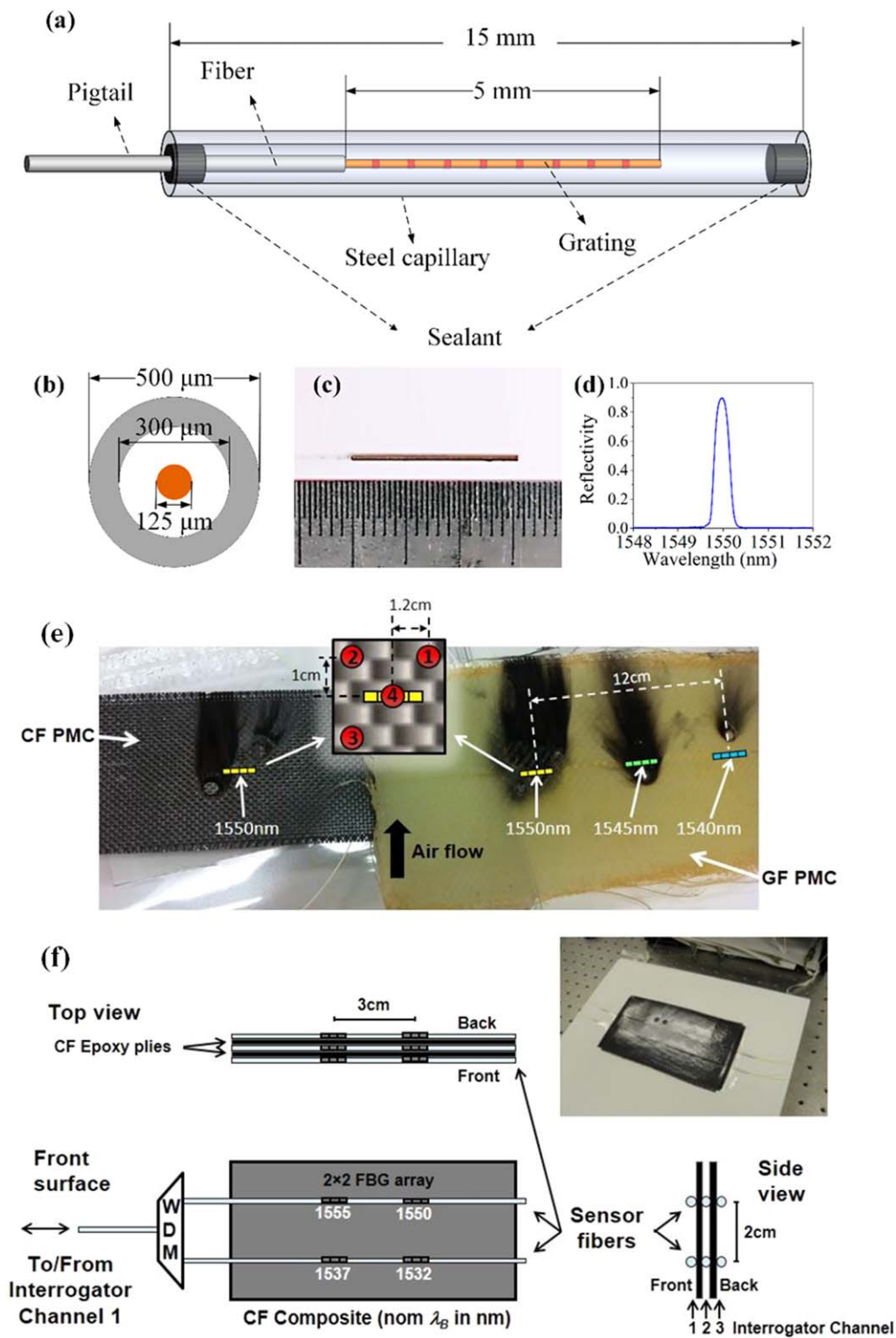


Figure 10. (a) Schematic, (b) cross section, (c) photo of the encapsulated FBG (EFBG) sensor and (d) typical reflection spectrum. Reproduced from [57] under the Creative Commons Attribution 4.0 International (CC BY 4.0) Licence. (e) Polymer matrix composite (PMC) specimens tested for their high-temperature response. Sensor positions in each PMC are indicated by their nominal Bragg wavelength. Air flow to remove smoke was upwards across each composite (CF: carbon fibre; GF: E-glass fibre). (f) Test setup used to measure the response of a $2 \times 2 \times 3$ array of sensors embedded on the surface and between two plies of CF composite. The nominal Bragg wavelengths of the FBGs are as shown. The actual composite specimen is shown in the upper-right corner. Reproduced from [58] under the Creative Commons Attribution 4.0 International (CC BY 4.0) Licence.

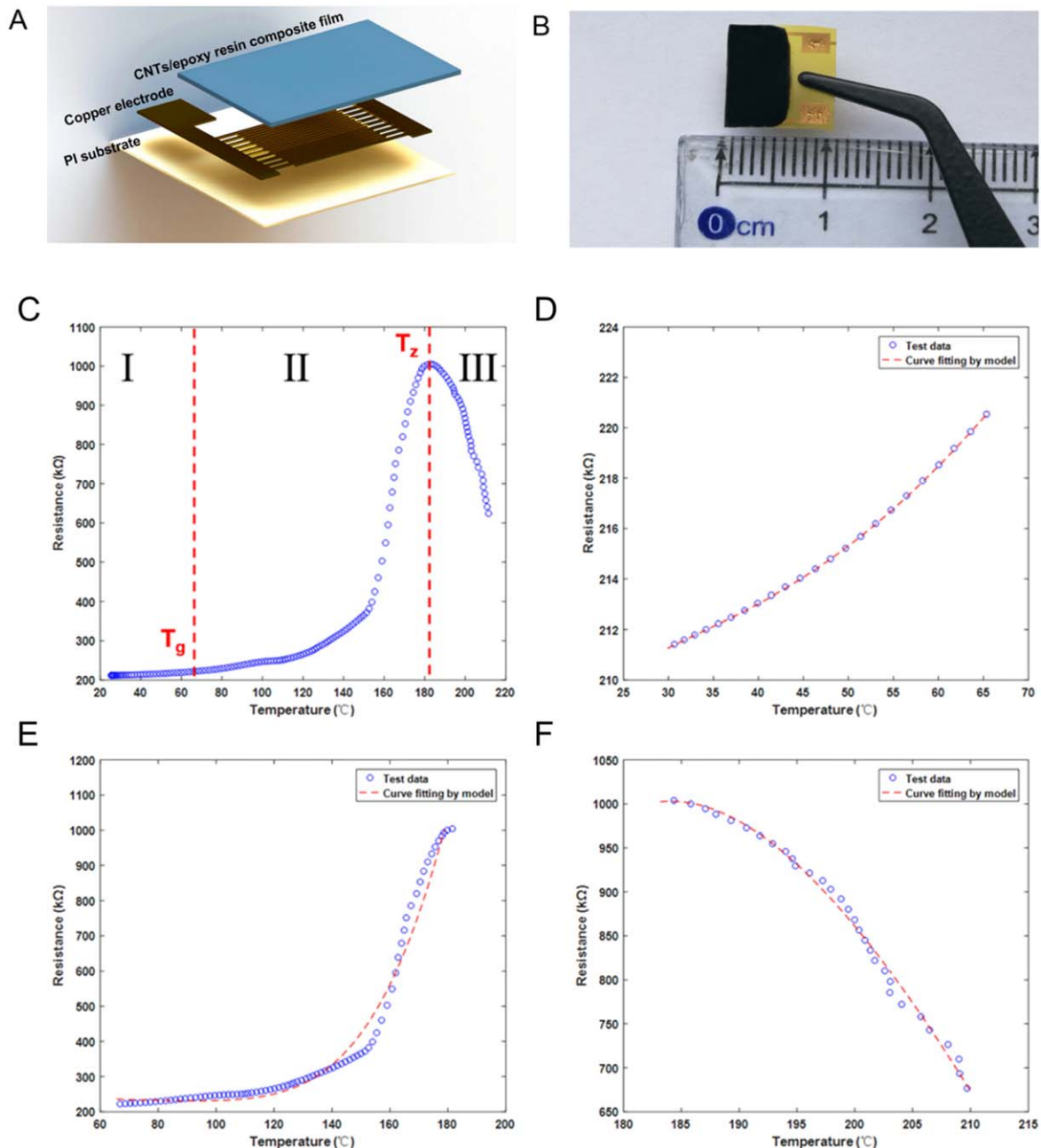


Figure 11. (A) Illustration of the three-layer structure of the sensor. The bottom layer is the flexible PI substrate. The intermediate layer is a copper electrode coated with a $1\ \mu\text{m}$ thick gold film. The top layer is the MWCNT/epoxy resin CPC film with a thickness of $50\ \mu\text{m}$. (B) Photograph of an assembled sensor prototype (For interpretation of the references to colour in this figure legend, the reader is referred to the web version of this article). (C) Resistance–temperature characteristics of MWCNT/epoxy resin CPC measured between $20\ ^\circ\text{C}$ and $210\ ^\circ\text{C}$. The overall curve was divided into three stages: (D) below the glass transformation temperature (T_g); (E) between T_g and T_z (the transition temperature of PTC and NTC) and (F) above T_z . The segmented equation matched the experimental data for each stage. Reproduced with permission from [35]. Copyright 2019 Elsevier.

materials science. Wang *et al.*, demonstrated Raman spectroscopy-based temperature sensors using functionalised multiwalled carbon nanotubes (MWCNTs) and epoxy resin composite films that with integrated Cu electrodes (figures 11(A)–(B)) [35]. The temperature change, which was measured by using Raman spectroscopy, was correlated with the change in strain value of MWCNTs depending on temperature. Flexible polyimide (PI) substrates were deposited with Cu electrodes by sputtering. Then, the sensing materials

were printed to have a thickness of $50\ \mu\text{m}$ (figure 10(a)). The temperature sensors showed high sensitivity in the range of $20\ ^\circ\text{C}$ – $210\ ^\circ\text{C}$ (figures 11(C)–(F)).

Fluorescence-based sensors use a length of optical fibre that is coated with a temperature-sensitive material. As temperature changes, the material emits light at a different wavelength, which can be measured to determine the temperature. Fluorescence-based sensors are highly sensitive and can be used in applications such as biomedical imaging and

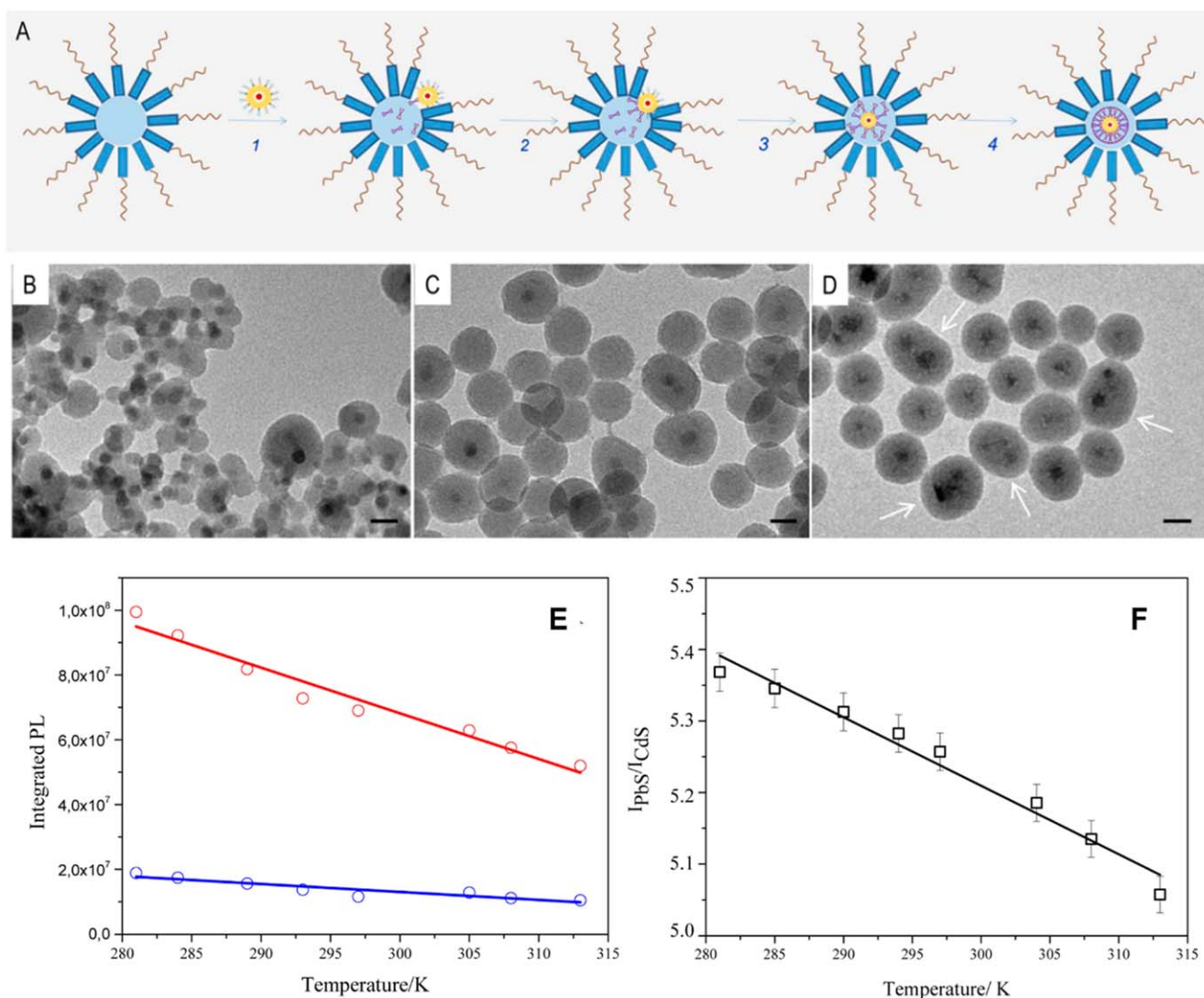


Figure 12. (A) Scheme of the water-in-oil microemulsion approach for silica shell growth: addition of the organic-capped GQDs to the water-in-oil microemulsion (step 1), displacement of the native ligands at the quantum dot (QD) surface by surfactant molecules and hydrolysed TEOS (step 2), inclusion of the surface modified QDs inside the water pool of the inverse micelle (step 3) and formation of the siloxane network around the QDs (step 4). Transmission electron microscopy micrographs (scale bar: 50 nm) of silica nanostructures prepared using native GQDs (B) and oleyl amine-treated GQDs under increasing volume of GQDs: 30 μL (C) and 80 μL (D). The reaction mixture consists of 350 μL Igepal CO-520, 200 μL NH_4OH , 50 μL TEOS and 30 μL APTS. The reaction is allowed to proceed overnight at 28 $^\circ\text{C}$. The arrows used in panel D highlight the elongated multicore structures (32% yield). Scatter plot and line fit of (E) integrated fluorescence of CdS (blue symbol and line, I_{CdS}) and PbS (red symbol and line, I_{PbS}) versus temperature and (F) ratiometric response ($I_{\text{PbS}}/I_{\text{CdS}}$) versus temperature. Reproduced from [59] under the Creative Commons Attribution 4.0 International (CC BY 4.0) Licence.

environmental monitoring. Fanizza *et al* utilised fluorescent nanomaterials including silica nanoparticles, organic-capped PbS@CdS@CdS ‘giant’ quantum dots (GQDs) for the accurate temperature sensors (figures 12(A)–(D)) [59]. Uniform and single-core silica-coated GQD (GQD@SiO₂) nanoparticles exhibited temperature-dependent fluorescent spectra in the range of 281–313 K (figures 12(e)–(f)), which confirmed the potential of PbS@CdS@CdS-based temperature sensors for futuristic biomedical devices.

SPR sensors use a length of optical fibre that is coated with a thin layer of metal. As temperature changes, the metal layer undergoes a change in refractive index, causing a shift in the resonance wavelength of the surface plasmon waves (figures 13(a)–(d)). By measuring this wavelength shift, the

temperature can be determined. SPR sensors are highly sensitive and can be used in applications such as food safety and environmental monitoring. Song *et al*, demonstrated a temperature sensor based on SPR with a TiO₂–Au–TiO₂ triple structure (figures 13(e)–(f)) [60]. The excitation of SPR was possible by both Au and TiO₂ in the triple combination structure of TiO₂ and Au. Thus, they could achieve a highly sensitive SPR temperature sensor exhibiting a sensitivity of 6038.53 nm RIU⁻¹ and the detection temperature sensitivity of $-2.40 \text{ nm } ^\circ\text{C}^{-1}$ (figures 13(g)–(h)). These values were 77.81% higher than those of traditional Au SPR sensors.

Clad modified fibre optic sensors use nanostructures coated cladding modified fibre (CMF). CMF based sensors are easy to fabricate, less weight, and have good durability.

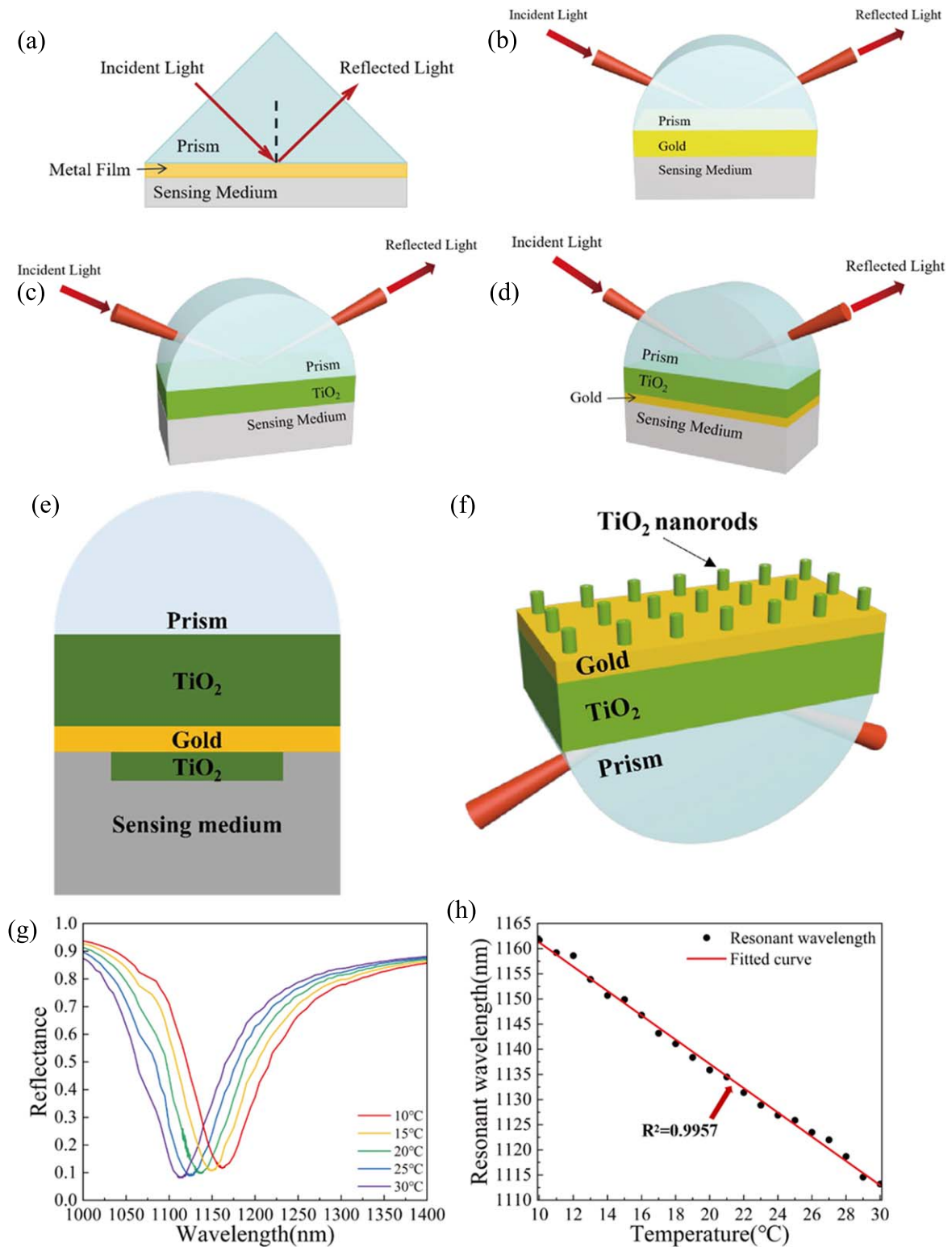


Figure 13. (a) Schematic of the Kretschmann configuration. (b) Schematic of a pure gold (Au) SPR sensor. (c) Schematic of a pure titanium dioxide (TiO₂) SPR sensor. (d) Schematic of the proposed TiO₂-Au dual-structure SPR sensor. Schematic of the TiO₂(film)-Au-TiO₂(nanorods) triple structure SPR sensor: (e) two-dimensional and (f) 3D. (g) Reflectance curve of the optimised TiO₂(film)-Au-TiO₂(nanorods) triple SPR sensor in the 10 °C–30 °C range and (h) SPR wavelength corresponding to temperature for every 1 °C in the 10 °C–30 °C range and linear fitting. Reproduced from [60] under the Creative Commons Attribution 4.0 International (CC BY 4.0) Licence.

CMF is made by removing a small portion of the cladding using the chemical etching method and coating it with semiconductor metal oxide in its place. When light is projected onto the temperature sensor, some of the light passes

through because the refractive index of the modified cladding and the core are different. The refractive index of the modified cladding material changes as the temperature changes, and the intensity of the light also changes accordingly. By measuring

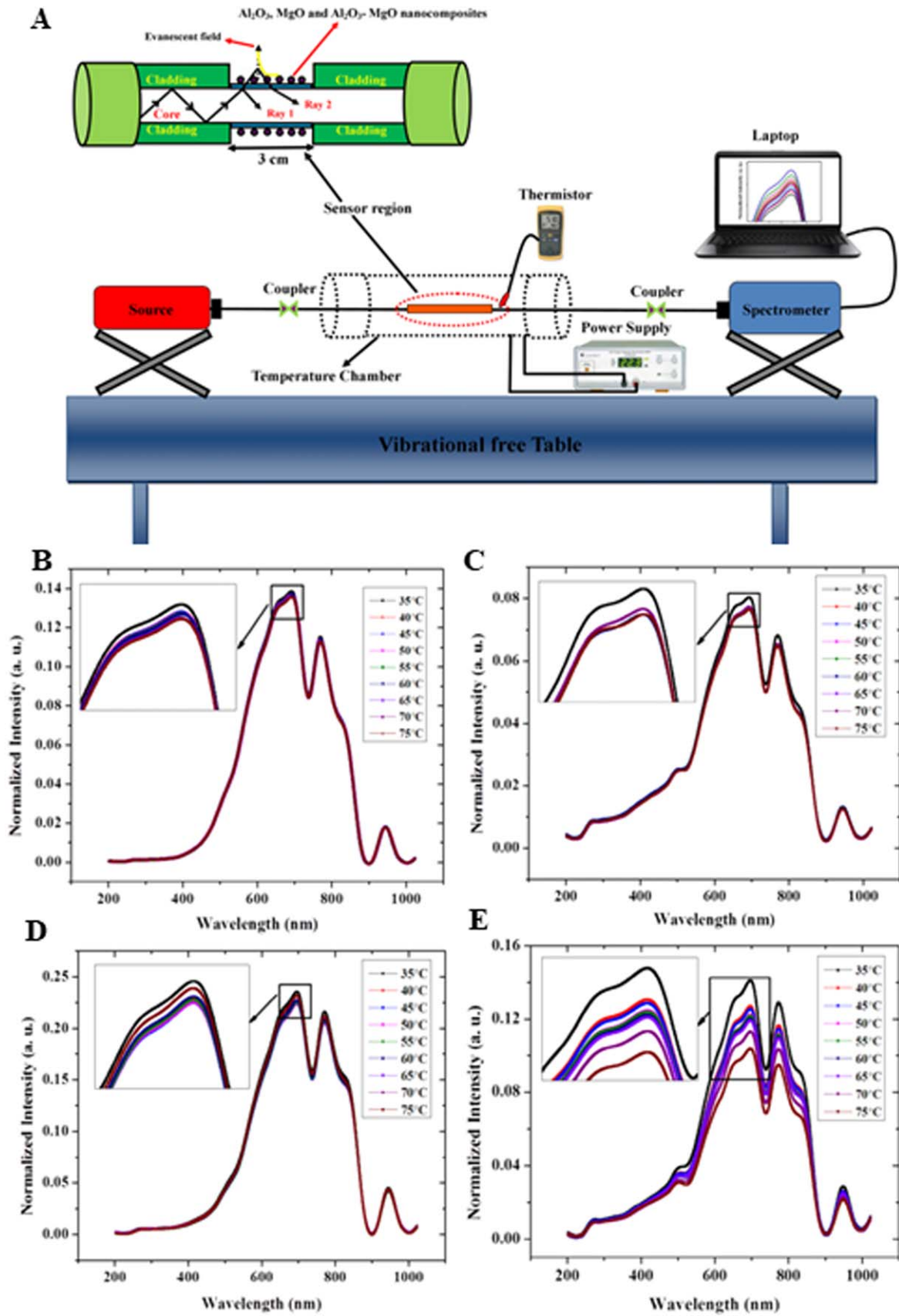


Figure 14. (A) Schematic diagram of the fibre optic temperature sensor setup. Reproduced from [62]. Copyright 2018 IOP Publishing Ltd (B–E) Spectral response of nanopowders (B) ZnO (C) SnO_2 (D) TiO_2 and (E) Al_2O_3 for temperature (35 °C to 75 °C) at 697 nm. Reproduced from [61]. Copyright 2019 Elsevier.

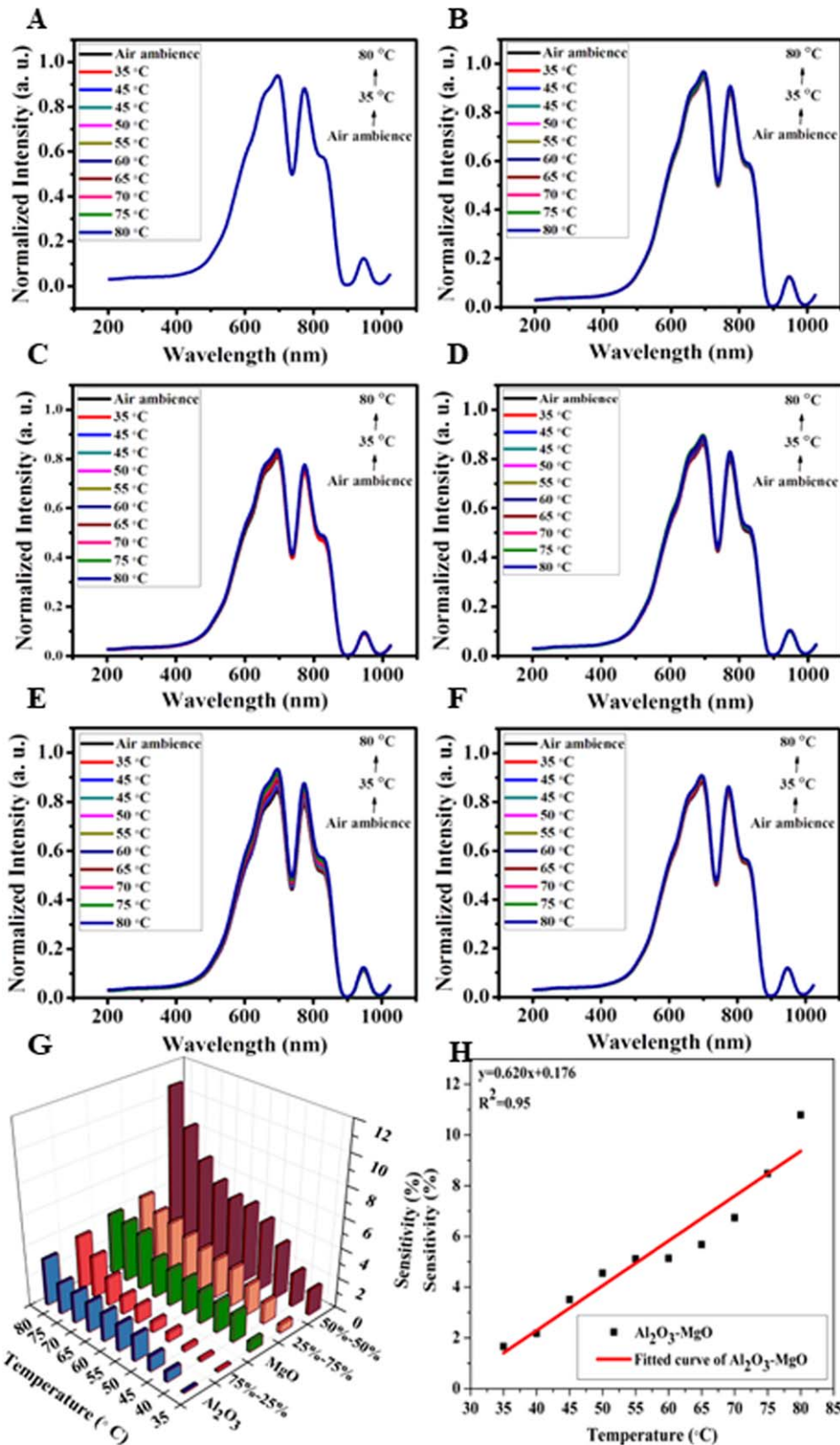


Figure 15. (A-F) Spectral response of the temperature sensors at different temperature range of 35 °C–80 °C (A) bare fibre (B) Al₂O₃ (C) MgO (D) Al₂O₃-MgO (25%–75%) (E) Al₂O₃-MgO (50%–50%) and (F) Al₂O₃-MgO (75%–25%). (G) Temperature sensitivity of Al₂O₃, Al₂O₃-MgO (75%–25%), MgO, Al₂O₃-MgO (25%–75%), Al₂O₃-MgO (50%–50%) nanoparticles at the wavelength of 693 nm. (H) Relationship between temperature and sensitivity of Al₂O₃-MgO (50%–50%). Reproduced from [62]. Copyright 2019 Elsevier.

the light intensity, the temperature can be determined (figure 14(A)). Narasimman *et al.*, made clad modified fibre sensors with various metal oxide nanoparticles (ZnO, SnO₂, TiO₂, and Al₂O₃) [61]. When the sensitivity was measured at a wavelength of 697 nm, the performance of Al₂O₃ was about 27, showing superior characteristics compared to other materials. The sensitivity was higher when measured with a blue LED (figures 14(B)–(E)). In the other work by Narasimman *et al.*, the Al₂O₃-MgO nanocomposite based clad modified fibre sensor was demonstrated [62]. The performance of the sensor was evaluated by varying the content of Al₂O₃ and MgO (figures 15(A)–(G)). It can be seen that the sensitivity of the Al₂O₃-MgO (50%–50%) nanocomposite-based sensor was higher than other composites. The temperature and sensitivity had linear relationships which measured as 0.62%/°C in the case of the Al₂O₃-MgO (50%–50%) nanocomposite-based sensor (figure 15(H)).

Overall, fibre optic temperature sensors provide several advantages over traditional temperature sensors, including high accuracy, fast response times and immunity to electromagnetic interference. The progression of the fibre optic sensors will facilitate the realisation of the futuristic wearable devices having the function of temperature monitoring. A comparison of the features of fibre optic temperature sensors is shown in table 3.

3. Conclusion

In summary, textile-based temperature sensors have shown great promise for a wide range of applications. Recent developments have resulted in various sensor types, each offering benefits over traditional temperature sensors, such as flexibility, conformability and comfort for the wearer. The integration of these sensors into fabric-based products enables continuous temperature monitoring, making them ideal for medical and fitness applications. Researchers have explored different types of fibre-based temperature sensors, including resistive, thermoelectric and fibre-optical sensors, all of which demonstrate good sensitivity in temperature monitoring. However, there are still challenges to overcome, such as improving sensitivity and accuracy, integrating wireless communication capabilities and developing low-cost fabrication techniques. In addition, textile-based temperature sensors must have durability and reliability to withstand various mechanical stresses and should be configured so that temperature sensing is not affected by electronic components. Therefore, further research and development is necessary to address the issues and innovate the conventional textile-based temperature sensors. For that, further optimization of the design, fabrication and integration methods to integrate the sensors into textile products and development of novel materials and sensing technologies to improve the accuracy and sensitivity are required. An interdisciplinary approach among material science, textile engineering, and electronics is also needed. In summary, continuous innovation and advancement in materials, fabrication methods, design, calibration methods, and signal processing are essential for

overcoming these challenges. The continued efforts and progress to innovate the fibre-based temperature sensors will revolutionize wearable device industry requiring sensitive temperature monitoring system.

Acknowledgments

We gratefully acknowledge financial support from the National Research Foundation (NRF) of Korea, which is funded by the Ministry of Science, Information and Communications Technology (Grant Nos. NRF-2021K1A3A1A74096164 and NRF-2022K1A3A1A39089566). This work was supported by funding from Bavarian Center for Battery Technology (BayBatt), Bayerisch-Tschechische Hochschulagentur (BTHA) (BTHA-AP-2022-45, BTHA-AP-2023-5, and BTHA-AP-2023-12). This work was also supported by the University of Bayreuth-Deakin University Joint Ph.D. Program, Bayerische Forschungallianz (BayFOR) (BayIntAn_UBT_2023_84), and collaboration project funding from Kangwon National University and LINC 3.0 Research Center. This research was supported by ‘Research Base Construction Fund Support Program’ funded by Jeonbuk National University in 2023.

Data availability statement


All data that support the findings of this study are included within the article (and any supplementary files).

Conflicts of interest

The authors declare that they have no competing interests.

ORCID iDs

Sooman Lim  <https://orcid.org/0000-0002-7336-5081>

Jun Young Cheong  <https://orcid.org/0000-0002-4999-3264>

Byungil Hwang  <https://orcid.org/0000-0001-9270-9014>

References

- [1] Li Y *et al* 2009 Metal coating of fiber bragg grating and the temperature sensing character after metallization *Opt. Fiber Technol.* **15** 391–7
- [2] Lin C C *et al* 2013 Performance enhancement of metal-oxide-semiconductor tunneling temperature sensors with nanoscale oxides by employing ultrathin Al₂O₃ high-k dielectrics *Nanoscale* **5** 8090–7
- [3] Ballato J *et al* 2004 A ceramic photonic crystal temperature sensor *J. Am. Ceram. Soc.* **82** 2273–5
- [4] Yurddaskal M *et al* 2017 Carbon black and graphite filled conducting nanocomposite films for temperature sensor applications *J. Mater. Sci., Mater. Electron.* **28** 9514–8

- [5] Davaji B *et al* 2017 A patterned single layer graphene resistance temperature sensor *Sci. Rep.* **7** 8811
- [6] Di Bartolomeo A *et al* 2009 Multiwalled carbon nanotube films as small-sized temperature sensors *J. Appl. Phys.* **105** 064518
- [7] Chuang H-S *et al* 2009 Design, fabrication and characterization of a conducting PDMS for microheaters and temperature sensors *J. Micromech. Microeng.* **19** 045010
- [8] Kinkeldei T *et al* 2009 Development and evaluation of temperature sensors for textile integration *Sensors* **15** 80–3
- [9] Sahatiya P *et al* 2016 Graphene-based wearable temperature sensor and infrared photodetector on a flexible polyimide substrate *Flex. Print. Electron.* **1** 025006
- [10] Kumari S *et al* 2013 Optical and structural characterization of pulsed laser deposited ruby thin films for temperature sensing application *Appl. Surf. Sci.* **265** 180–6
- [11] Dankoco M D *et al* 2016 Temperature sensor realized by inkjet printing process on flexible substrate *Mater. Sci. Eng. B* **205** 1–5
- [12] Zhang P *et al* 2021 Fiber-based thermoelectric materials and devices for wearable electronics *Micromachines* **12** 869
- [13] Noh J-S 2016 Conductive elastomers for stretchable electronics, sensors and energy harvesters *Polymers* **8** 123
- [14] Xie S 2022 The design considerations and challenges in MOS-based temperature sensors: a review *Electronics* **11** 1019
- [15] Ramakrishnan M *et al* 2016 Overview of fiber optic sensor technologies for strain/temperature sensing applications in composite materials *Sensors* **16** 99
- [16] Liu G *et al* 2018 A flexible temperature sensor based on reduced graphene oxide for robot skin used in internet of things *Sensors* **18** 1400
- [17] Husain M D *et al* 2013 Preliminary investigations into the development of textile based temperature sensor for healthcare applications *Fibers* **1** 2–10
- [18] Kim J-H *et al* 2022 On-wafer temperature monitoring sensor for condition monitoring of repaired electrostatic chuck *Electronics* **11** 880
- [19] Kim S 2020 Inkjet-printed electronics on paper for RF identification (RFID) and sensing *Electronics* **9** 1636
- [20] Zeng W *et al* 2022 Temperature sensing shape morphing antenna (ShMoA) *Micromachines* **13** 1673
- [21] Ghosh A *et al* 2023 Applications of smart material sensors and soft electronics in healthcare wearables for better user compliance *Micromachines* **14** 121
- [22] Al-Qahtani A M *et al* 2023 Performance optimization of wearable printed human body temperature sensor based on silver interdigitated electrode and carbon-sensing film *Sensors* **23** 1869
- [23] Manfredi R *et al* 2023 Long-term stability in electronic properties of textile organic electrochemical transistors for integrated applications *Materials* **16** 1861
- [24] Ye X *et al* 2022 All-fabric-based flexible capacitive sensors with pressure detection and non-contact instruction capability *Coatings* **12** 302
- [25] Lee J-W *et al* 2018 PEDOT:PSS-based temperature-detection thread for wearable devices *Sensors* **18** 2996
- [26] Kan C-W *et al* 2021 Future trend in wearable electronics in the textile industry *Appl. Sci.* **11** 3914
- [27] Afroj S *et al* 2021 Multifunctional graphene-based wearable e-textiles *Proceedings* **68** 11
- [28] Landsiedel J *et al* 2021 Multi-point flexible temperature sensor array and thermoelectric generator made from copper-coated textiles *Sensors* **21** 3742
- [29] Acar G *et al* 2019 Wearable and flexible textile electrodes for biopotential signal monitoring: a review *Electronics* **8** 479
- [30] Zaman S *et al* 2022 Smart e-textile systems: a review for healthcare applications *Electronics* **11** 99
- [31] Wiklund J *et al* 2021 A review on printed electronics: fabrication methods, inks, substrates, applications and environmental impacts *J. Manuf. Mater. Process.* **5** 89
- [32] Qu K-A *et al* 2022 A mini-review on preparation of functional composite fibers and their based devices *Coatings* **12** 473
- [33] Kang M *et al* 2021 Recent advances in fiber-shaped electronic devices for wearable applications *Appl. Sci.* **11** 6131
- [34] Su Y *et al* 2020 Printable, highly sensitive flexible temperature sensors for human body temperature monitoring: a review *Nanoscale Res. Lett.* **15** 200
- [35] Wang W *et al* 2019 Raman spectroscopy and resistance-temperature studies of functionalized multiwalled carbon nanotubes/epoxy resin composite film *Microelectron. Eng.* **214** 50–4
- [36] Xiang Z *et al* 2019 Multifunctional textile platform for fiber optic wearable temperature-monitoring application *Micromachines* **10** 866
- [37] Heo J S *et al* 2020 Challenges in design and fabrication of flexible/stretchable carbon- and textile-based wearable sensors for health monitoring: a critical review *Sensors* **20** 3927
- [38] Stavarakis A K *et al* 2021 Electrical characterization of conductive threads for textile electronics *Electronics* **10** 967
- [39] Khan S *et al* 2019 Recent developments in printing flexible and wearable sensing electronics for healthcare applications *Sensors* **19** 1230
- [40] Wu S 2022 An overview of hierarchical design of textile-based sensor in wearable electronics *Crystals* **12** 555
- [41] Hughes-Riley T *et al* 2018 A historical review of the development of electronic textiles *Fibers* **6** 34
- [42] Blachowicz T *et al* 2021 Textile-based sensors for biosignal detection and monitoring *Sensors* **21** 6042
- [43] Fernández-Caramés T M *et al* 2018 Towards the internet of smart clothing: a review on iot wearables and garments for creating intelligent connected e-textiles *Electronics* **7** 405
- [44] Lu Z *et al* 2022 A stable and durable triboelectric nanogenerator for speed skating land training monitoring *Electronics* **11** 3717
- [45] Shyamkumar P *et al* 2014 Wearable wireless cardiovascular monitoring using textile-based nanosensor and nanomaterial systems *Electronics* **3** 504–20
- [46] Angelucci A *et al* 2021 Smart textiles and sensorized garments for physiological monitoring: a review of available solutions and techniques *Sensors* **21** 814
- [47] Chatterjee K *et al* 2021 Thermoelectric materials for textile applications *Molecules* **26** 3154
- [48] Liu D *et al* 2021 Screen-printed flexible thermoelectric device based on hybrid silver selenide/PVP composite films *Nanomaterials* **11** 2042
- [49] Liu Z *et al* 2021 High-performance temperature sensor by employing screen printing technology *Micromachines* **12** 924
- [50] Li M *et al* 2020 Large-area, wearable, self-powered pressure-temperature sensor based on 3d thermoelectric spacer fabric *ACS Sens.* **5** 2545–54
- [51] Zhang T *et al* 2019 Ultraflexible glassy semiconductor fibers for thermal sensing and positioning *ACS Appl. Mater. Interfaces* **11** 2441–7
- [52] Lugoda P *et al* 2020 Flexible temperature sensor integration into e-textiles using different industrial yarn fabrication processes *Sensors* **20** 73
- [53] Xiao S *et al* 2008 A novel fabrication process of MEMS devices on polyimide flexible substrates *Microelectron. Eng.* **85** 45–7
- [54] Lee C-Y *et al* 2008 Fabrication of micro sensors on a flexible substrate *Sensors Actuators A* **147** 173–6

- [55] Liu S *et al* 2022 Self-powered multi-parameter sensing system without decoupling algorithm needed based on flexible triboelectric nanogenerator *Nano Energy* **104** 107889
- [56] Fromme N P *et al* 2021 Metal-textile laser welding for wearable sensors applications *Adv. Electron. Mater.* **7** 2001238
- [57] Chen C *et al* 2020 Hybrid temperature and stress monitoring of woven fabric thermoplastic composite using fiber bragg grating based sensing technique *Sensors* **20** 3081
- [58] Jenkins R B *et al* 2017 Localized temperature variations in laser-irradiated composites with embedded fiber bragg grating sensors *Sensors* **17** 251
- [59] Fanizza E *et al* 2020 Encapsulation of dual emitting giant quantum dots in silica nanoparticles for optical ratiometric temperature nanosensors *Appl. Sci.* **10** 2767
- [60] Song Y *et al* 2022 Temperature sensor based on surface plasmon resonance with TiO₂-Au-TiO₂ triple structure *Materials* **15** 7766
- [61] Narasimman S *et al* 2019 Fabrication of fiber optic based temperature sensor *Mater. Today Proc.* **9** 164–74
- [62] Narasimman S *et al* 2018 Al₂O₃-MgO nanocomposite based fiber optic temperature sensor *Mater. Res. Express* **5** 115014